

Analysis and Synthesis of Switched Optimization Algorithms^{*}

Jared Miller^{*} Fabian Jakob^{**} Carsten Scherer^{*}
Andrea Iannelli^{**}

^{*} *Chair of Mathematical Systems Theory, Department of Mathematics, University of Stuttgart, Stuttgart, Germany (e-mail: {jared.miller, carsten.scherer}@imng.uni-stuttgart.de).*

^{**} *Institute for Systems Theory and Automatic Control, University of Stuttgart, Germany (e-mail: {fabian.jakob, andrea.iannelli}@ist.uni-stuttgart.de).*

Abstract Deployment of optimization algorithms on networked systems face challenges associated with time delays and corruptions. One particular instance is the presence of time-varying delays arising from factors such as packet drops and irregular sampling. Fixed time delays can destabilize gradient descent algorithms, and this degradation is exacerbated by time-varying delays. This work concentrates on the analysis and creation of discrete-time optimization algorithms with certified exponential convergence rates that are robust against switched uncertainties between the optimizer and the gradient oracle. These optimization algorithms are implemented by a switch-scheduled output feedback controllers. Rate variation and sawtooth behavior (packet drops) in time-varying delays can be imposed through constraining switching sequences. Analysis is accomplished by bisection in the convergence rate to find Zames-Falb filter coefficients. Synthesis is performed by alternating between a filter coefficient search for a fixed controller, and a controller search for fixed multipliers.

Keywords: Networked systems, Control of switched systems, Static optimization problems, Convex optimization, Robust control, Control over networks, Systems with time-delays.

1. INTRODUCTION

Optimization algorithms increasingly operate within networked environments, where information exchange is rarely perfect. Communication links introduce delays, packet drops, and other distortions that alter how optimization algorithms interact with their gradient oracles. These effects can have significant consequences – slowing convergence, degrading performance, or even destabilizing the algorithm dynamics.

In the strongly convex setting, robust control techniques have been used to analyze and synthesize optimization algorithms. Introduced by Lessard et al. (2016), the essential idea is to treat first-order algorithms as Lur’e systems, and to frame the convergence as an absolute stability problem. Uncertainties arising in the gradient oracle are described using Integral Quadratic Constraints (IQCs) (Megretski and Rantzer, 1997; Boczar et al., 2018), and the design of robust algorithms can subsequently be cast as a controller synthesis problem (Scherer and Ebenbauer, 2021). This methodology enables to quantify robustness to gradient perturbations in terms of H_2 performance (Michalowsky

et al., 2021; Mohammadi et al., 2021), or to account for adversarial communication dynamics by considering them within an extremum control setup (Holicki and Scherer, 2021).

Most of this system-theoretic approach has focused on time-invariant algorithm and network dynamics (Scherer and Ebenbauer, 2021; Scherer et al., 2023). Even though recently this approach was extended to time-varying objectives and algorithms in (Jakob and Iannelli, 2025), important network-induced phenomena such as *time-varying delays* have not been specifically addressed yet. When such effects are taken into account, the resulting dynamics are more accurately captured by switched or hybrid systems (Wen’an et al., 2008; Conte et al., 2020).

Motivated by this perspective, this work extends the system-theoretic framework to include *switched optimization algorithms*. The design of optimization algorithms in a switched setting has mostly focused on analysis and synthesis of distributed algorithms that are robust against time-varying information delays in the form of stale gradients (Ramaswamy et al., 2021; Bianchi et al., 2021; Doostmohammadian et al., 2021). Delay-scheduled algorithms, in analogy to delay-scheduled controllers (Briat et al., 2009), have not yet been addressed.

This work performs analysis of switched optimization algorithms by solving linear matrix inequality frameworks over O’Shea-Zames-Falb IQCs (Scherer, 2023) using parameter-

^{*} J. Miller and C. Scherer are supported by the Deutsche Forschungsgemeinschaft (DFG, German Research Foundation) under Germany’s Excellence Strategy - EXC 2075 - 390740016. We acknowledge the support by the Stuttgart Center for Simulation Science (SimTech). F. Jakob acknowledges the support of the International Max Planck Research School for Intelligent Systems (IMPRS-IS).

affine (Apkarian et al., 1995) and path-dependent (Ahmadi et al., 2014) storage functions. The switched optimization synthesis problem is posed as a robustness requirement under a regulation constraint (Francis and Wonham, 1976; Stoorvogel et al., 2000) compatible under parameter/mode changes (Köröglu and Scherer, 2008; Köröglu, 2012; Conte et al., 2021). Given fixed multipliers, we perform switched optimization algorithm synthesis by applying nonlinear transformation techniques for LPV systems (De Caigny et al., 2012) using the extended characterization of (De Oliveira et al., 2002). The convergence rates and empirical performance of the resulting algorithms are demonstrated on switching delay models and case studies.

The contributions of this work are:

- A switched-system framework for accelerated first-order algorithms with bilateral corrupted gradient transmission, encompassing error models such as packet dropout and bounded-rate delay.
- An analysis procedure for upper-bounding worst-case convergence rates of given switched optimization algorithms.
- An internal-model-control-based synthesis procedure in the polytopic LPV setting for minimal worst-case linear convergence under switched network dynamics.

The paper has the following structure: Section 2 reviews preliminaries about notation, optimization properties, switched systems, and time-varying delay. Section 3 formulates the switched optimization algorithm analysis and synthesis problems. Section 4 performs analysis of switched optimization algorithms based on antipassivity conditions. Section 5 synthesizes mode-dependent output-feedback controllers such that the feedback interconnection between the controller and the network forms a switched optimization algorithm. Section 6 presents numerical examples demonstrating the efficacy of our approach. Section 7 concludes the paper and outlines areas of future research.

Notation. The set of natural numbers including 0 is \mathbb{N} . For $a, b \in \mathbb{N}$ we denote the integer interval from a to b (inclusive) by $a..b$. An \mathbb{R}^n -valued signal is a map $x : \mathbb{N} \rightarrow \mathbb{R}^n$. The one-step shift operator is \mathbf{z} . Given an initial condition $x_0 \in \mathbb{R}^n$ a linear system is a signal mapping $u \rightarrow y$ described by

$$y = \begin{bmatrix} A & B \\ C & D \end{bmatrix} u, \quad \begin{aligned} x_{k+1} &= Ax_k + Bu_k \\ y_k &= Cx_k + Du_k. \end{aligned} \quad (1)$$

Given two linear systems $G_1 : (q, z) \rightarrow (p, w)$ and $G_2 : (w, u) \rightarrow (z, y)$, we denote the star product $G_1 \star G_2 : (q, u) \rightarrow (p, y)$ as the well-posed feedback interconnection of G_1 and G_2 along the common channels w and z .

The symbol $e_i \in \mathbb{R}^n$ will denote the standard unit vector. Positive (semi)-definiteness of a symmetric matrix P will be denoted as $P \succ 0$ ($P \succeq 0$). The identity matrix of dimension n is I_n . The zeros and all-ones matrices of dimension $m \times n$ are $0_{m \times n}$ and $1_{m \times n}$, respectively. Canonical transpose elements in a symmetric matrix or a quadratic form may be substituted by an asterisk $*$.

Given a directed graph $\mathcal{G} = \{\mathcal{V}, \mathcal{E}\}$ with vertices \mathcal{V} and edges \mathcal{E} (with the possibility of self-loops) and the set of all infinite-length paths in \mathcal{G} is $\text{Path}(\mathcal{G})$.

2. PRELIMINARIES

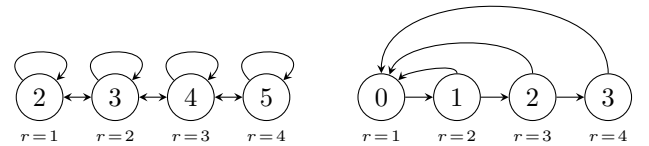
2.1 Switched Systems

An switched system with exogenous switching signal s with n states, n_u inputs, and n_y outputs is described by

$$\begin{aligned} x_{k+1} &= A_{s_k} x_k + B_{s_k} u_k \\ y_k &= C_{s_k} x_k + D_{s_k} u_k. \end{aligned} \quad (2)$$

In this work, we assume that (2) includes N_s -subsystems, and that the tuple (n, n_u, n_y) is the same between all subsystems. A trajectory of (2) is defined with respect to a switching function $s : \mathbb{N} \rightarrow 1..N_s$ as $\{(s_k, x_k)\}_k$, in which each pair (x_k, x_{k+1}) obeys (2) under the active subsystem s_k . An external switching logic will be encoded by demanding $s \in \text{Path}(\mathcal{G})$ for some switching graph $\mathcal{G} = \{\mathcal{V}, \mathcal{E}\}$, where the vertices $r \in \mathcal{V}$ are labeled with the modes $r = 1..N_s$ and the edges \mathcal{E} define the transitions $r \rightarrow r'$ that can be performed.

One concrete example of switched optimization algorithms is in the case of time-varying network delays. Example graphs \mathcal{G} associated to two time-varying delays models are shown in Figure 1. Figure 1a shows a graph encoding delays that can take values $s_k \in 2..5$, with a bounded rate of change $|s_{k+1} - s_k| \leq 1$. The vertices Figure 1b describes the packet drop case as a reset system: the delay s_k either increases by one (packet drop) or snaps to 0 (successful packet transmission) up to a maximum delay of 3.



(a) Bounded rate delay.

(b) Packet drop.

Figure 1. Examples of directed switching graphs \mathcal{G} for different models of time-varying delay.

Time-varying delays within a range of 0 and H_{\max} can be mapped to a switched system with (Conte et al., 2020) modes $r \in 1..H_{\max}$ as

$$\begin{aligned} A_r^d &= \begin{bmatrix} 0_{1 \times H_{\max}-1} & 0 \\ I_{H_{\max}-1} & 0_{H_{\max}-1 \times 1} \end{bmatrix} & B_r^d &= \begin{bmatrix} 1 \\ 0_{1 \times H_{\max}-1} \end{bmatrix} \\ C_r^d &= \begin{cases} 0_{1 \times H_{\max}-1}, & r = 1 \\ e_r^\top, & r \neq 1 \end{cases} & D_r^d &= \begin{cases} 1, & r = 1 \\ 0, & r \neq 1. \end{cases} \end{aligned} \quad (3)$$

For example, a variable delay s taking values in $s_k \in \{0, 1, 2\}$ can be represented as the switched system

$$\left(\begin{array}{cc} A_r^d & B_r^d \\ C_r^d & D_r^d \end{array} \right)_{r=1}^3 = \left(\left(\begin{array}{cc} 0 & 0 \\ 1 & 0 \end{array} \right), \left(\begin{array}{cc} 0 & 0 \\ 1 & 0 \end{array} \right), \left(\begin{array}{cc} 0 & 0 \\ 0 & 1 \end{array} \right) \right).$$

2.2 Stability and Robustness of Switched Systems

An autonomous switched system $x_{k+1} = A_{s_k} x_k$ is internally exponentially stable at rate ρ if there exists a

constant $\gamma > 0$, such that for all switching sequences $s \in \text{Path}(\mathcal{G})$ and initial points $x_0 \in \mathbb{R}^n$, it holds

$$\|x_k\|_2 \leq \gamma \rho^k \|x_0\|_2. \quad (4)$$

Relation (4) implies that $x_{k+1} = (1/\rho') A_{s_k} x_k$ is Lyapunov stable (joint spectral radius < 1 (Gripenberg, 1996)) for all $\rho' > \rho$. The system in (2) satisfies an ϵ -strictly anti-passivity property for $\epsilon > 0$ under arbitrary $s \in \text{Path}(\mathcal{G})$ if and only if positive definite storage functions $V_r : \mathbb{R}^n \rightarrow \mathbb{R}_{\geq 0}$ for each mode $r \in 1..N_s$ exists such that

$$V_{s_T}(x_T) - V_{s_0}(x_0) < -\sum_{k=0}^{T-1} u_k^\top y_k - \epsilon \|u_k\|_2^2 \quad (5)$$

The condition in (5) can also be expressed as a dissipation relation holding for all $\tilde{x} \in \mathbb{R}^{n_x}$, $\tilde{u} \in \mathbb{R}^{n_u}$:

$$\forall (r, r') \in \mathcal{E} : V_{r'}(A_r \tilde{x} + B_r \tilde{u}) - V_r(\tilde{x}) < -\tilde{u}^\top \tilde{y} - \epsilon \|\tilde{u}\|_2^2, \quad (6)$$

which when restricting to quadratic storage functions $V_r(\tilde{x}) = \tilde{x}^\top M_r \tilde{x}$, $M_r \succ 0$ yields the condition $\forall (r, r') \in \mathcal{E}$:

$$[*]^\top \begin{bmatrix} M_r & 0 \\ 0 & -M_{r'} \end{bmatrix} \begin{bmatrix} A_r & B_r \\ I & 0 \end{bmatrix} + [*]^\top \begin{bmatrix} 0 & I \\ I & -\epsilon I \end{bmatrix} \begin{bmatrix} C_r & D_r \\ 0 & I \end{bmatrix} \prec 0. \quad (7)$$

3. PROBLEM FORMULATION

The optimization problem under consideration is to solve

$$f^* = \min_{z \in \mathbb{R}^d} f(z). \quad (8)$$

The function f is m -strongly convex and L -Lipschitz with $0 < m < L < \infty$, in the following denoted as $f \in \mathcal{S}_{m,L}$. The unique optimal solution of (8) is denoted by z^* , i.e., $\nabla f(z^*) = 0$. The set $\mathcal{S}_{m,L}^0 \subset \mathcal{S}_{m,L}$ is the class of functions $f \in \mathcal{S}_{m,L}$ such that $f(0) = 0, \nabla f(0) = 0$. The optimization task in (8) takes place in a networked setting, in which the optimizer can only interact with the gradient oracle ∇f remotely.

The overall networked optimization involves a discrete-time switched network model. For each fixed mode $r \in 1..N_s$, the network evolves as

$$P_r : \begin{bmatrix} x_{k+1} \\ z_k \\ y_k \end{bmatrix} = \begin{bmatrix} A_r & B_{r,1} & B_{r,2} \\ C_{r,1} & D_{r,11} & D_{r,12} \\ C_{r,2} & D_{r,21} & D_{r,22} \end{bmatrix} \begin{bmatrix} x_k \\ w_k \\ u_k \end{bmatrix}. \quad (9a)$$

The network will be interconnected with a switched controller that parametrizes the optimization algorithm. For each mode r , the controller evolves as

$$K_r : \begin{bmatrix} \xi_{k+1} \\ u_k \end{bmatrix} = \begin{bmatrix} A_r^K & B_r^K \\ C_r^K & D_r^K \end{bmatrix} \begin{bmatrix} \xi_k \\ y_k \end{bmatrix}, \quad (9b)$$

with internal state ξ_k . The resulting optimization algorithm for each mode r is the interconnection $P_r \star K_r$ with augmented state $\zeta_k = [x_k; \xi_k]$, which for each r evolves as

$$P_r \star K_r : \begin{bmatrix} \zeta_{k+1} \\ z_k \end{bmatrix} = \begin{bmatrix} \tilde{A}_r & \tilde{B}_r \\ \tilde{C}_r & 0 \end{bmatrix} \begin{bmatrix} \zeta_k \\ w_k \end{bmatrix}. \quad (9c)$$

The deployment of the optimization algorithm (9c) w.r.t. an oracle ∇f and a switching sequence $\{s_k\} \in \text{Path}(\mathcal{G})$ is

$$\begin{bmatrix} \zeta_{k+1} \\ z_k \end{bmatrix} = \begin{bmatrix} \tilde{A}_{s_k} & \tilde{B}_{s_k} \\ \tilde{C}_{s_k} & 0 \end{bmatrix} \begin{bmatrix} \zeta_k \\ w_k \end{bmatrix}, \quad w_k = \nabla f(z_k). \quad (10)$$

Figure (2) visualizes the interconnection of $\nabla f, P_r, K_r$ with respect to an external switching signal $s \in \text{Path}(\mathcal{G})$.

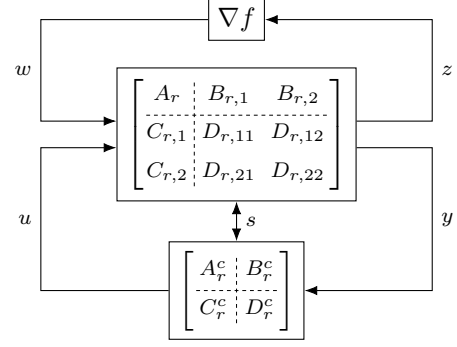


Figure 2. A switch-scheduled first-order method. A switching signal s determines which mode r at each k .

The system in (9c) is a feasible optimization algorithm if $w_k \rightarrow 0, z_k \rightarrow z^*$ for any initial condition ζ_0 and any admissible switching sequence s . It is furthermore exponentially convergent at rate ρ if there exists a constant $\gamma_z > 0$ such that for all $s \in \text{Path}(\mathcal{G})$ it holds that

$$\|z_k - z^*\|_2 \leq \gamma_z \rho^k \|z_0 - z^*\|_2. \quad (11)$$

We pose the following two problems:

Problem 1. (Analysis). Given $f \in \mathcal{S}_{m,L}$, an algorithm $P_r \star K_r$ (9c), and a switching graph \mathcal{G} , find an infimal ρ such that (11) holds given the algorithm deployment in (10).

Problem 2. (Synthesis). Given $f \in \mathcal{S}_{m,L}$, a network model P_r as in (9a), and a switching graph \mathcal{G} , formulate an r -dependent output feedback controller K_r such that $P_r \star K_r$ forms a feasible optimization algorithm with infimal ρ .

The following assumptions are made:

Assumption 1. The function f is a member of $\mathcal{S}_{m,L}$.

Assumption 2. The function f is independent of the switching index r .

Assumption 3. The graph \mathcal{G} is finite ($N_s < \infty$).

Assumption 4. For every vertex $r \in \mathcal{V}$, there exists a vertex r' such that r' lies on a cycle of \mathcal{G} , and r' is reachable by a path from r .

Assumption 1 restricts the structure of the considered nonlinearities ∇f , and ensures that a unique fixed optimizer z^* exists for the optimization problem. Assumption 2 ensures that the function f is static and independent of the network. Assumptions 3 and 4 are conditions ensuring that infinite-length paths exist in the finite graph \mathcal{G} .

4. OPTIMIZATION ALGORITHM ANALYSIS

We begin by performing analysis of switched optimization algorithms. The infimal rate ρ^* solving Problem 1 will be bounded by bisection over ρ . At each fixed ρ value, we will search over causal O'Shea-Zames-Falb multipliers to certify ρ -convergence of the switched optimization algorithm.

4.1 Structural Regulation

We first describe a regulation property (Francis and Wonham, 1976; Wen'an et al., 2008) that is sufficient to ensure that trajectories of (9c) converge to an optimal point z^* . Proving convergence to z^* will be based on a transformation to error coordinates e with error-objective f^0 :

$$e := z - z^* \quad f^0(e) := f(e + z^*). \quad (12)$$

Theorem 3. A sufficient condition for an algorithmic interconnection (10) to converge to an optimal solution z^* for any $s \in \text{Path}(\mathcal{G})$, $f \in \mathcal{S}_{m,L}$ is that there exists vectors $(\Theta_r)_{r=1}^{N_s}$ such that

$$\forall(r, r') \in \mathcal{E} : \quad \tilde{A}_r \Theta_r - \Theta_{r'} = 0, \quad (13a)$$

$$\forall r \in 1..N_r : \quad \tilde{C}_r \Theta_r = I \quad (13b)$$

and that the following Lur e interconnection is asymptotically stable as $\lim_{k \rightarrow \infty} (v_k, e_k) \rightarrow (0, 0)$ for all $f^0 \in \mathcal{S}_{m,L}^0$, $s \in \text{Path}(\mathcal{G})$:

$$v_{k+1} = \tilde{A}_{s_k} v_k + \tilde{B}_{s_k} w_k \quad (14a)$$

$$e_k = \tilde{C}_{s_k} v_k \quad (14b)$$

$$w_k = \nabla f^0(e_k) \quad (14c)$$

Proof. Viewing $\eta = z^*$ as a constant exogenous input, the algorithm deployment in (10) can be posed as

$$\eta_{k+1} = \eta_k, \quad \eta_0 = z^* \quad (15a)$$

$$x_{k+1} = \tilde{A}_s x_k + \tilde{B}_s w_k \quad (15b)$$

$$e_k = \tilde{C}_s x_k - \eta_k \quad (15c)$$

$$w_k = \nabla f^0(e_k). \quad (15d)$$

We note that (13) is a particular instance of a regulator equation in a switching setting (Francis and Wonham, 1976; Conte et al., 2021). After introducing a new state v_k with $v_k := x_k - \Theta_{s_k} \eta_k$, the expression in (15) becomes

$$\eta_{k+1} = \eta_k, \quad \eta_0 = z^* \quad (16a)$$

$$v_{k+1} = \tilde{A}_{s_k} v_k + \tilde{B}_{s_k} w_k + (\tilde{A}_k \Theta_{s_k} - \Theta_{s_{k+1}}) \eta_k \quad (16b)$$

$$e_k = \tilde{C}_{s_k} v_k + (\tilde{C}_{s_k} \Theta_{s_k} - I) \eta_k \quad (16c)$$

$$w_k = \nabla f^0(e_k). \quad (16d)$$

Satisfaction of (13) therefore decouples the disturbance η from the v dynamics and the e output channel. If the v -dynamics Lur e system is stable as $\lim_{k \rightarrow \infty} v_k = 0$ for all $s \in \text{Path}(\mathcal{G})$, then output regulation is achieved because $\lim_{k \rightarrow \infty} e_k = \lim_{k \rightarrow \infty} \tilde{C}_{s_k} v_k = 0$.

Theorem 3 certifies asymptotic stability. We now provide a sufficient condition for ρ -exponential stability of (10) based on the interconnection of an exponentially transformed system in (2) with a static time-varying map

$$\bar{F}(k, z) = \rho^{-k} \nabla f^0(\rho^k z). \quad (17)$$

Corollary 4. A sufficient condition for the algorithm in (9c) to be ρ -convergent to z^* as in (11) is if the condition (13) holds and the following system is Lyapunov stable for all $s \in \text{Path}(\mathcal{G})$, $f^0 \in \mathcal{S}_{m,L}^0$:

$$\bar{v}_{k+1} = (\rho^{-1} \tilde{A}_{s_k}) \bar{v}_k + (\rho^{-1} \tilde{B}_{s_k}) \bar{w}_k \quad (18a)$$

$$\bar{e}_k = \tilde{C}_{s_k} \bar{v}_k \quad (18b)$$

$$\bar{w}_k = \bar{F}(k, \bar{e}_k) \quad (18c)$$

Proof. This proof follows arguments from (Scherer, 2023) about exponential stability. Let $\mathcal{T}_{\rho^{-1}}$ denote the ρ -exponential signal weighting map, transforming a sequence v into

$$\mathcal{T}_{\rho^{-1}} : (v_0, v_1, v_2, \dots) \mapsto (v_0, \rho^{-1} v_1, \rho^{-2} v_2, \dots). \quad (19)$$

Defining the exponentially weighted signals $\bar{v} = \mathcal{T}_{\rho^{-1}} v$, $\bar{e} = \mathcal{T}_{\rho^{-1}} e$, $\bar{w} = \mathcal{T}_{\rho^{-1}} w$, we note that Lyapunov stability of \bar{v} implies exponential stability of the unweighted signal v ($\exists K : \|\bar{v}_k\|_2 \leq K \|\bar{v}_0\|_2 \implies \|v_k\|_2 \leq K \rho^{-k} \|v_0\|_2$) (Desoer and Vidyasagar, 1975).

4.2 Multiplier-Based Analysis

Members of $\mathcal{S}_{m,L}^0$ satisfy a family of dissipation relations:

Lemma 5. (Lemma 5 of (Scherer et al., 2023)). Consider a function $f^0 \in \mathcal{S}_{m,L}^0$, an exponential rate $\rho \in (0, 1]$, and a sequence of filter coefficients $\{\lambda_\nu\}_{\nu=0}^{\nu_{\max}}$ satisfying

$$\lambda_\nu \leq 0 \quad \forall \nu \geq 1, \quad \sum_{\nu=0}^{\nu_{\max}} \rho^{-\nu} \lambda_\nu > 0. \quad (20)$$

Define respective m and L weightings of the ρ -weighted nonlinearity

$$\bar{F}_m(k, z) := \bar{F}(k, z) - mz, \quad (21a)$$

$$\bar{F}^L(k, z) := Lz - \bar{F}(k, z). \quad (21b)$$

For any sequence z , define the exponentially weighted sequences $\bar{z}, \bar{p}, \bar{q}, \bar{g}$ as

$$\bar{z}_k := \rho^{-k} z_k \quad \bar{q}_k := \bar{F}_m(k, \bar{z}_k) \quad (22a)$$

$$\bar{p}_k := \bar{F}^L(k, \bar{z}_k) \quad \bar{g}_k := \sum_{\nu=0}^k \lambda_\nu \bar{p}_{k-\nu}. \quad (22b)$$

The sequences \bar{q}, \bar{g} then satisfy a dissipation relation

$$\forall T > 0 \quad \sum_{k=0}^{T-1} \bar{q}_k^\top \bar{g}_k \geq 0. \quad (23)$$

The choice of $\lambda_0 = 1, \lambda_{\geq 1} = 0$ leads to a passivity property (identity multiplier). Cases with $\lambda_{\geq 1} \neq 0$ describe dynamic multipliers. For a given set of filter coefficients λ , fixed matrices A_f, B_f , and λ -affine maps C_f, D_f , we denote the state space realization of the filter described by λ as

$$\begin{bmatrix} \bar{x}_{k+1}^f \\ \bar{g}_k \end{bmatrix} = \begin{bmatrix} A_f & B_f \\ C_f(\lambda) & D_f(\lambda) \end{bmatrix} \begin{bmatrix} \bar{x}_k^f \\ \bar{q}_k \end{bmatrix}. \quad (24)$$

In order to apply Lemma 5 to prove exponential stability of the algorithm (9c), we must conduct signal transformation to match the form of (21):

$$\begin{bmatrix} \bar{p}_k \\ \bar{q}_k \end{bmatrix} = \begin{bmatrix} L & -1 \\ 1 & -m \end{bmatrix} \begin{bmatrix} \bar{w}_k \\ \bar{z}_k \end{bmatrix} \Leftrightarrow \begin{bmatrix} \bar{p}_k \\ \bar{w}_k \end{bmatrix} = \begin{bmatrix} L - m & 1 \\ 1 & m \end{bmatrix} \begin{bmatrix} \bar{q}_k \\ \bar{z}_k \end{bmatrix}. \quad (25)$$

The signal transformation via (25) of the per-mode exponentially weighted algorithm (9c) is

$$\begin{pmatrix} \hat{A}_r & \hat{B}_r \\ \hat{C}_r & \hat{D}_r \end{pmatrix} = \begin{pmatrix} \rho^{-1}(\tilde{A}_r + \tilde{B}_r m \tilde{C}_r) & \rho^{-1} \tilde{B}_r \\ (L - m) \tilde{C}_r & -1 \end{pmatrix}. \quad (26)$$

The cascade connection between the transformed system (26) and the filter λ is

$$\begin{pmatrix} \hat{A}_r^\lambda & \hat{B}_r^\lambda \\ \hat{C}_r^\lambda & \hat{D}_r^\lambda \end{pmatrix} = \begin{pmatrix} A_f & B_f \hat{C}_r & D_f(\lambda) \hat{B}_r \\ 0 & \hat{A}_r & B_\lambda \\ C_f(\lambda) & C_f(\lambda) \hat{C}_r & D_f(\lambda) \hat{D}_r \end{pmatrix}. \quad (27)$$

Theorem 6. Under Assumptions 1-4, the switched algorithm $P_r \star K_r = (\tilde{A}_r, \tilde{B}_r, \tilde{C}_r)_r$ from (9c) is certified as ρ -exponentially convergent for any $s \in \text{Path}(\mathcal{G})$ if the condition in (13) is satisfied and the following program is feasible for fixed filter order ν_{\max} and tolerance $\epsilon > 0$:

$$\text{find}_{M, \lambda} \quad \forall s \in 1..N_s : M_s \succ 0 \quad (28a)$$

$$\forall(r, r') \in \mathcal{E} : \quad (28b)$$

$$\begin{aligned} & [\star]^\top \begin{bmatrix} M_r & 0 \\ 0 & -M_{r'} \end{bmatrix} \begin{bmatrix} \hat{A}_r^\lambda & \hat{B}_r^\lambda \\ I & 0 \end{bmatrix} \\ & + [\star]^\top \begin{bmatrix} 0 & I \\ I & -\epsilon I \end{bmatrix} \begin{bmatrix} \hat{C}_r^\lambda & \hat{D}_r^\lambda \\ 0 & I \end{bmatrix} \prec 0 \end{aligned} \quad (28c)$$

$$\lambda \in \mathbb{R}^{\nu_{\max}} \text{ under (20)}. \quad (28d)$$

Proof. The equation in (28c) enforces ϵ -strict antipassivity of the system in (7) (ρ -weighting, loop formation, interconnection with λ). Lemma 5 details that all elements of class $\mathcal{S}_{m,L}^0$ are passive under this sequence of transformations via the dissipation relation (23). Because the interconnection between a strictly antipassive system and a passive system is exponentially stable, feasibility of (28) ensures that the system in (9c) is ρ -stable for all members of $\mathcal{S}_{m,L}^0$ Scherer et al. (2023). Theorem 3 ensures that stability under $\mathcal{S}_{m,L}^0$ interconnection and the satisfaction of regulation (13) by assumption implies convergence to the fixed point z^* for all $f \in \mathcal{S}_{m,L}$.

The problem in (28) is a finite-dimensional convex program for fixed ρ and filter order ν_{\max} . Exponential performance of \tilde{G} can be upper-bounded by performing bisection on ρ . The accuracy of the bound can be increased by increasing ν_{\max} , but there is no guarantee of convergence to the true rate bound.

5. ALGORITHM SYNTHESIS

We now focus on the synthesis of switching optimization methods. The regulation property from Theorem 3 will be guaranteed through the introduction of an internal model.

The algorithm synthesis problem with fixed filter λ satisfying (20) and convergence bound ρ is as follows:

Problem 7. Given a function class $\mathcal{S}_{m,L}$, a network P_r from (9a), a switching graph \mathcal{G} , and a multiplier $\lambda \in \mathbb{R}^{\nu_{\max}}$ satisfying (20), create a controller (9b) K_r such that $P_r \star K_r$ is ρ -exponentially convergent for any $s \in \text{Path}(\mathcal{G})$.

5.1 Regulation

In order to apply the regulation framework to generate controllers, we make an assumption based on the solvability of an open-loop regulation equation:

Assumption 5. Given matrices $(A_r, B_{r,2}, C_{r,2}, D_{r,12})$ from the dynamics P_r in (9a), there exists a solution $\Pi_r \in \mathbb{R}^{n \times 1}$, $\Gamma_r \in \mathbb{R}$ for the following regulator equation

$$\forall(r, r') \in \mathcal{E} : \quad A_r \Pi_r + B_{r,2} \Gamma_r = \Pi_{r'} \quad (29a)$$

$$C_{r,2} \Pi_r + D_{r,12} \Gamma_r = -I. \quad (29b)$$

Validity of (5) allows us to construct a controller such that the regulation property (29) will be satisfied by construction. Given a solution (Π_r, Γ_r) to (29), we define the following per-mode feedback matrix

$$\Phi_r = C_{r,2} \Pi_r + D_{r,12} \Gamma_r. \quad (30)$$

A per-mode internal model inspired by (Stoorvogel et al., 2000) (originally derived for a non-switched system) is

$$Q_r : \quad \begin{bmatrix} \omega_{k+1} \\ u_k \\ \tilde{y}_k \end{bmatrix} = \begin{bmatrix} I & 0 & I & 0 \\ -\Gamma_r & 0 & 0 & I \\ \Phi_r & I & 0 & 0 \end{bmatrix} \begin{bmatrix} \omega_k \\ y_k \\ \tilde{u}_{1k} \\ \tilde{u}_{2k} \end{bmatrix}. \quad (31)$$

We restrict the control synthesis task to the design of subcontrollers in interconnection with $P_r \star Q_r$

$$R_r : \quad \begin{bmatrix} \tilde{\xi}_{k+1} \\ \tilde{y}_k \end{bmatrix} = \begin{bmatrix} A_{r,c} & B_{r,c} \\ C_{r,c1} & D_{r,c1} \\ C_{r,c2} & D_{r,c2} \end{bmatrix} \begin{bmatrix} \tilde{\xi}_k \\ \tilde{u}_{1,k} \\ \tilde{u}_{2,k} \end{bmatrix} \quad (32)$$

such that controller K_r (9b) can be expressed as the interconnection $K_r = Q_r \star R_r$ (31) and (32) with

$$K_r : \quad \begin{bmatrix} A_r^K & B_r^K \\ C_r^K & D_r^K \end{bmatrix} = \begin{bmatrix} I + D_{r,c1} \Phi_r & C_{r,c1} & D_{r,c1} \\ B_{r,c} \Phi_r & A_{r,c} & B_{r,c} \\ -\Gamma_r + D_{r,c2} \Phi_r & C_{r,c2} & D_{r,c2} \end{bmatrix}. \quad (33)$$

The following structure constraint ensures that there are no algebraic loops in the evaluation of ∇f :

$$D_{r,12} \neq 0 \implies D_{r,c2} = 0 \quad (34)$$

Theorem 8. If Assumption 5 is satisfied, then the controller structure (33) ensures that $P_r \star Q_r \star R_r$ satisfies condition (29) for output regulation from Theorem 3.

Proof. This follows from standard arguments in regulator theory from (Francis and Wonham, 1976) with respect to the model structure in (Stoorvogel et al., 2000). The algorithm $P_r \star Q_r \star R_r$ has plant matrices with $\tilde{D}_r = 0$ of

$$\tilde{A}_r = \begin{bmatrix} A_r + B_{r,2} D_{r,c2} C_{r,2} & -B_{r,2} (\Gamma_r - D_{r,c2} \Phi_r) & B_{r,2} C_{r,c2} \\ D_{r,c1} C_{r,2} & I + D_{r,c1} \Phi_r & C_{r,c1} \\ B_{r,c} C_{r,2} & -B_{r,c} \Phi_r & I - A_{r,c} \end{bmatrix}$$

$$\tilde{B}_r = \begin{bmatrix} B_{r,1} \\ D_{r,c1} D_{r,11} \\ B_{r,c} D_{r,11} \end{bmatrix}, \quad \tilde{C}_r = \begin{bmatrix} (C_{r,1} + D_{r,12} D_{r,c2} C_{r,2})^\top \\ (-D_{r,12} (\Gamma_r - D_{r,c2} \Phi_r))^\top \\ (D_{r,12} C_{r,c2})^\top \end{bmatrix}^\top \quad (35)$$

Choosing $\Theta_r = [-\Pi_r^\top, I, 0]^\top$ and $\Theta_{r'} = [-\Pi_{r'}^\top, I, 0]^\top$ yields

$$\begin{bmatrix} \tilde{A}_r \\ \tilde{C}_r \end{bmatrix} \Theta_r - \Theta_{r'} = \begin{bmatrix} \Pi_{r'} - A_r \Pi - B_{r,2} \Gamma_r \\ -D_{r,c1} (C_{r,2} \Pi_r - (C_{r,2} \Pi_r)) \\ -B_{r,c1} (C_{r,2} \Pi_r - (C_{r,2} \Pi_r)) \\ -(C_{r,1} \Pi_r + D_{r,12} \Gamma_r) \end{bmatrix} \quad (36)$$

$$= [0; 0; 0; I]. \quad (37)$$

The step from (36) to (37) is taken by applying relation (29) and constraint (34). The Theorem is therefore proven.

Example 9. Systems whose network dynamics are characterized by per-channel time-varying delay with maximal H_1^{\max} before ∇f and H_2^{\max} after ∇f will satisfy Assumption 5 with an r -independent solution of

$$\Pi = [1_{1 \times H_1^{\max}} \quad 0_{1 \times H_2^{\max}}] \otimes I_d \quad \Gamma = -I_d \quad \Phi = 0. \quad (38)$$

The resultant r -independent internal model is an integrator has an expression of

$$Q_r : \quad \begin{bmatrix} \omega_{k+1} \\ u_k \\ \tilde{y}_k \end{bmatrix} = \left(\begin{bmatrix} 1 & 0 & 1 & 0 \\ 1 & 0 & 0 & 1 \\ 0 & 1 & 0 & 0 \end{bmatrix} \otimes I_d \right) \begin{bmatrix} \omega_k \\ y_k \\ \tilde{u}_{1k} \\ \tilde{u}_{2k} \end{bmatrix}. \quad (39)$$

5.2 Controller Synthesis

In order to perform controller synthesis, we require the following assumption of well-posedness:

Assumption 6. For each $r \in 1..N_s$, it holds that $(I + D_{r,11} m)$ is invertible.

The interconnection between network dynamics (9a) and the internal model (31) for each $r \in 1..N_s$ is given by

$$\begin{bmatrix} \tilde{x}_{k+1} \\ \omega_{k+1} \\ z_k \\ \tilde{y}_k \end{bmatrix} = \begin{bmatrix} A_r & B_{r,1} & B_{r,1} & B_{r,2} & \Pi_r \\ 0 & I_d & 0 & 0 & I_d \\ C_{r,1} & D_{r,11} & D_{r,11} & D_{r,12} & 0 \\ C_{r,21} & D_{r,21} & D_{r,21} & D_{r,22} & 0 \end{bmatrix} \begin{bmatrix} \tilde{x}_k \\ \omega_k \\ w_k \\ \tilde{u}_{1,k} \\ \tilde{u}_{2,k} \end{bmatrix}. \quad (40)$$

The connection of the network dynamics and the per-mode internal model is

$$G_r = P_r \star Q_r = \begin{bmatrix} \hat{A}_r & \hat{B}_r \\ \hat{C}_r & \hat{D}_r \end{bmatrix}. \quad (41)$$

The controller synthesis problem can be posed as finding a sub-controller R_r ensuring that $P_r \star Q_r \star R_r$ is an optimization algorithm w.r.t. ∇f . The anti-passive formulation for controller synthesis given G_r, ρ, λ is to ensure that R_r from (32) renders a λ -filtered, loop-transformed, and exponentially weighted plant anti-passive (detailed in Appendix A). This antipassivity-restricted synthesis will be accomplished through the creation of r -dependent storage functions and nonlinear controller transformations. The controller synthesis and reconstruction procedure follows established methods for synthesis of LPV systems, refer to (De Caigny et al., 2012) for general concepts and to Appendix A for further detail. The alternating search between λ and R_r for controller synthesis is described in Algorithm 1.

Algorithm 1 Synthesis of Switched Optimization Algorithms

Require: A switching graph \mathcal{G} , a networked system P_r (9a), constants (m, L) , multiplier order ν_{\max} , number of iterations IterMax.

- 1: iter \leftarrow 1
 - 2: Initial static multiplier $\lambda \leftarrow 1$
 - 3: Compute internal models Q_r from (31)
 - 4: **for** iter $\in 1..\text{IterMax}$ **do**
 - 5: **Synthesis:** $(R_r) \leftarrow$ feasible subcontroller with infimal ρ under fixed multiplier λ given $P_r \star Q_r$.
 - 6: Recover the switched algorithm $(P_r \star Q_r \star R_r)$
 - 7: **Analysis:** $\lambda \leftarrow$ multiplier from Theorem 6 for analysis of $(P_r \star Q_r \star R_r)$ with infimal ρ
 - 8: **end for**
 - 9: **return** Algorithm $(P_r \star Q_r \star R_r)$, controller $(Q_r \star R_r)$, rate ρ , multiplier λ
-

6. NUMERICAL EXAMPLES

Numerical experiments are implemented in MATLAB (2024a). All LMIs are solved using LMIlab (Gahinet and Nemirovskii, 1993) from the Robust Control Toolbox of MATLAB. The code to generate experiments is publicly available at https://github.com/jarmill/time_var_opt. Plotted examples feature quadratic plus log-sum-exp functions for values $0 < m < L' < L < \infty$

$$f(z; Q, b) = \frac{1}{2} z^\top \Lambda z + b^\top z + (L - L') \log \left(\sum_{i=1}^d e^{z_i} + e^{-z_i} \right), \quad (42)$$

in which b is a randomly drawn vector in \mathbb{R}^d and Λ is a randomly generated symmetric matrix with eigenvalues between m and L . The function class (42) is inside $\mathcal{S}_{m,L}$.

6.1 Inhomogenous Networked System

We first consider minimization of f (42) over a network governed by $N_s = 4$ switching modes. The switching logic is displayed in Figure 3.

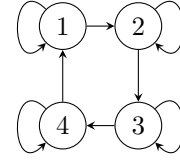


Figure 3. Ring-structured switching graph

The individual network dynamics in this scenario are

$$P_1^1 = \begin{bmatrix} 0 & \frac{1}{z-0.2} \\ -\frac{1}{z} & 0 \end{bmatrix}, \quad P_2^1 = \begin{bmatrix} 0 & \frac{1}{z-0.9} \\ -\frac{1}{2(z-0.2)} & 3 \end{bmatrix}, \\ P_3^1 = \begin{bmatrix} 0 & \frac{1}{z+0.5} \\ -\frac{1}{2(z-0.3)} & 0 \end{bmatrix}, \quad P_4^1 = \begin{bmatrix} 0 & \frac{1}{z+0.2} \\ -\frac{1}{z-1.2} & 3 \end{bmatrix}, \quad (43)$$

for which the full network dynamics are described by $P_r = P_r^1 \otimes I_d \forall r \in 1..N_s$.

The dynamics in (43) are chosen such that there exists unstable channel dynamics (in P_4^1) and that (29) admits a solution with non-identical Π and Γ values between modes. Figure 4 plots an upper-bound on the convergence rate developed by solving the analysis program (28) with FIR multipliers of order $\nu_{\max} = 3$. The reference algorithms are gradient descent and triple momentum (Van Scoy et al., 2017) with $\rho_{gd} = \frac{2}{m+L}$ and $\rho_{TM} = 1 - \sqrt{\frac{m}{L}}$ are tuned to optimally converge in the setting of $P = \begin{bmatrix} 0 & I \\ I & 0 \end{bmatrix}$. These algorithms have the expressions of

$$K_{gd} = \begin{bmatrix} 1 & -\frac{2}{m+L} \\ 1 & 0 \end{bmatrix} \otimes I_d \quad (44)$$

$$K_{TM} = \begin{bmatrix} 1 & 1 + \frac{\rho_{TM}^2}{2-\rho_{TM}} & -\frac{1+\rho_{TM}}{L} \\ 0 & \frac{\rho_{TM}^2}{2-\rho_{TM}} & \frac{1+\rho_{TM}}{L} \\ 1 & \frac{\rho_{TM}^2}{(1+\rho_{TM})(2-\rho_{TM})} & 0 \end{bmatrix} \otimes I_d, \quad (45)$$

The compared curves in Figure 4 are gradient descent, triple momentum, Synthesis under static multipliers ($\lambda = 1$), and Synthesis under static multipliers with the additional constraint that the storage function is common (the ring structure of switching is ignored). The path-dependent controller has a stability certificate of $\rho < 1$ when $L/m < 3.360$, and the common storage controller is stable with when $L/m < 1.660$. Gradient descent and triple momentum are both empirically unstable even when $m = 1, L = 1.01, L' = 1.005$.

The internal model (31) constructed from the solution to the regulator equation is parameterized by

$$\begin{bmatrix} \Gamma_r \\ \Phi_r \end{bmatrix} = \begin{bmatrix} -0.8 & -0.1 & -1.5 & -1.2 \\ 0 & -0.3 & -1.5 & -2.4 \end{bmatrix} \otimes I_d, \quad (46)$$

with a value of $\Pi_r = [0, 1]^\top \otimes I_d$ for all $r \in 1..4$.

We run Algorithm 1 for 3 iterations with Zames-Falb multipliers of order $\nu_{\max} = 3$. With only identity multipliers ($\lambda_0 = 1, \lambda_{\geq 1} = 0$), an order-3 controller (R_r) is obtained yielding $\bar{\rho} \leq 0.8944$. At the end of 3 iterations,

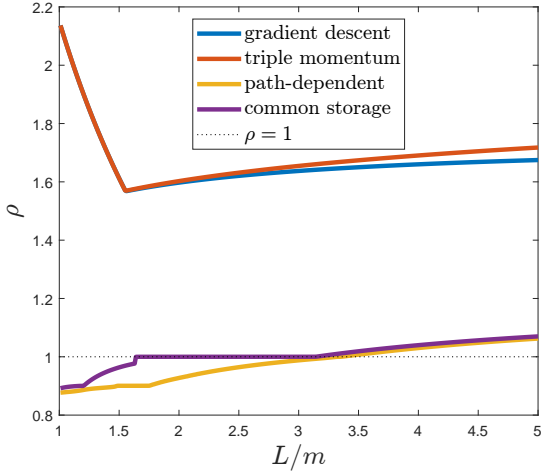


Figure 4. Analysis $\nu_{\max} = 3$ upper bounds on ρ

the Analysis routine certifies an order-6 controller (R_r) with $\rho \leq 0.8913$ under the multiplier $(\lambda_0, \lambda_1, \lambda_2, \lambda_3) = (1, -0.3922, -0.2977, -1.403 \times 10^{-6})$, $\lambda_{\geq 4} = 0$.

Figure 5 plots optimization of an instance of f over the network in (43) with $L' = 1.6$ by the developed controller.

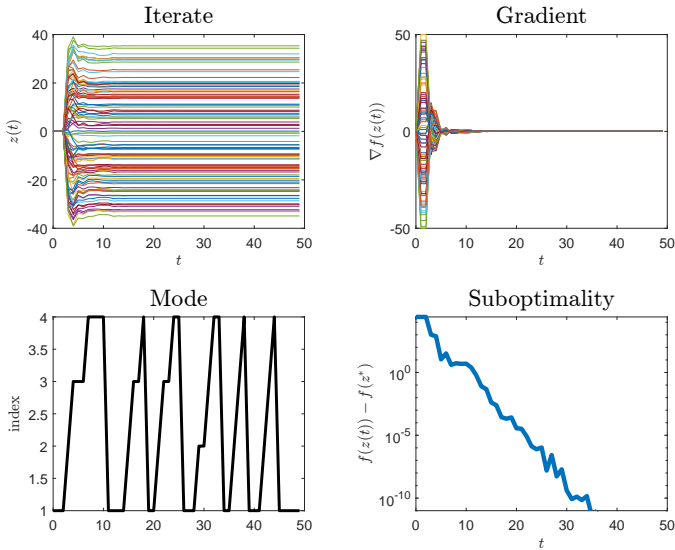


Figure 5. Algorithm execution with the $\rho = 0.8913$ controller

6.2 Time-Varying Delay: Increasing Delay

Our next example involves synthesis of algorithms with increasing delay before the oracle under snapping logic (delay increases by 1 until the maximum delay, or jumps to delay 0) visualized in Figure 1b. Figure 6 plots the computed convergence rate ρ under static multipliers λ for $m = 1$ and $L \in (1, 10]$. The maximal delay before the oracle increases from 0 to 6, and the upper-bound on the convergence rate ρ monotonically increases both in L/m and in the delay.

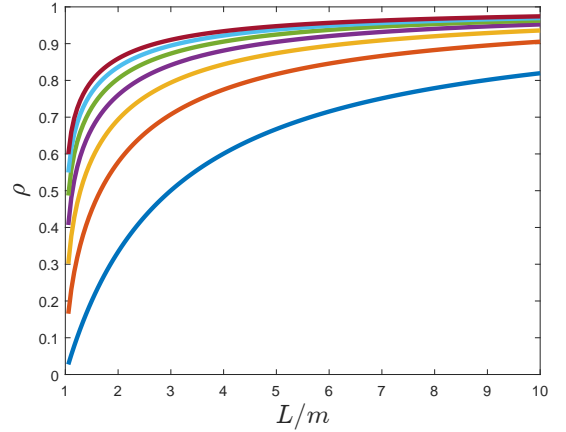


Figure 6. Rates under increasing delay and L

6.3 Time-Varying Delay: 3 step

Our last example involves synthesis of optimization algorithms under time-varying delay before the oracle with maximum delay 3. The function f is $\mu = 1$ strongly convex and has a Lipschitz constant within the range $L \in [1.5, 5]$. This experiment involves solving of Problem 2 for a fixed filter of $\lambda = 1$ under the following four \mathcal{G} -defining scenarios:

- (1) Delay changes by $\{-1, 0, 1\}$
- (2) Delay changes by $\{-2, -1, 0, 1, 2\}$
- (3) Delay increases by 1 (if delay < 3), or snaps to 0
- (4) Delay is unrestricted (arbitrary value in $\{0, 1, 2, 3\}$).

Figure 7 plots the computed ρ bounds with respect to these four scenarios. Scenarios 1-3 allow for switching-dependent storage functions as in (De Caigny et al., 2012). Scenario 4 (unrestricted switches) requires the existence of a common storage function (\mathcal{M}_s is independent of s). In this particular example, convergent algorithms are synthesized for all scenarios in the range of $L \in [1.4, 5]$. The convergence rate ρ satisfies a monotonic relation of $(1) \leq (2) \leq (4)$, as expected from removal of switching restrictions. In this case, the ‘snap’ scenario (3) has the smallest convergence rate. Furthermore all algorithms are convergent ($\rho < 1$). This monotonicity is retained in the range $(1, 5]$, but only the $[1.4, 5]$ subset is plotted in order to show this monotonicity.

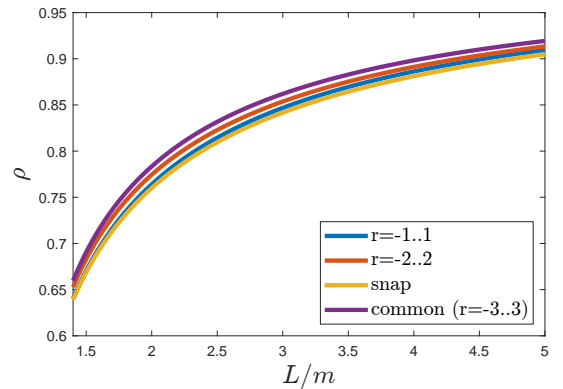


Figure 7. Rates under increasing L for maximum delay 3

7. CONCLUSION

This paper presented a delay-scheduled scheme to solve unconstrained optimization algorithms in the setting of time-varying discrete delays. The delay-scheduled optimization algorithm is posed as a (switched) family of linear systems, each of which are in Luré interconnection with the same gradient oracle (in class $\mathcal{S}_{m,L}$). Convergence to the algorithm's fixed point is accomplished if these systems jointly obey a discrete-time anti-passivity requirement over all possible switching transitions. Optimization algorithms can be analyzed through convex searches over Zames-Falb multiplier parameters. With fixed multipliers, delay-scheduled optimization algorithms can be synthesized through output feedback techniques. The analysis and synthesis tasks are jointly convex, and an alternating approach can be used to develop certified delay-scheduled algorithms with exponential convergence guarantees.

Future work involves the establishing of necessary conditions for switched internal models the finding of delay-scheduled controllers in the sampled data and unknown delay cases. Other work involves the formulating convex joint searches over controllers R_r and multipliers λ .

ACKNOWLEDGEMENTS

The authors would like to thank Zhiyu He, Chris Verhoek, Prof. Juan Francisco Camino, Prof. Roland Tóth, Jaap Eising, and Alessio Moreschini for discussions about switched systems and optimization algorithms.

Appendix A. CONTROLLER SYNTHESIS

This appendix demonstrates how the nonlinear transformation method from (De Caigny et al., 2012) for robust control of linear parameter varying systems can be used to synthesize switched optimization algorithms. The procedure of performing a ρ -transformation and applying the loop transformation in (21) to the system in (40) (similar to (26) for analysis) results in a system with state $\bar{\xi}$ as

$$\begin{bmatrix} \bar{\xi}_{k+1} \\ \bar{p}_k \\ \bar{y}_k \end{bmatrix} = \begin{bmatrix} A_r^\Delta & B_{r,1}^\Delta & B_{r,2}^\Delta \\ C_{r,1}^\Delta & D_{r,11}^\Delta & D_{r,12}^\Delta \\ C_{r,2}^\Delta & D_{r,21}^\Delta & D_{r,22}^\Delta \end{bmatrix} \begin{bmatrix} \bar{\xi}_k \\ \bar{q}_k \\ \bar{u}_k \end{bmatrix} \quad (\text{A.1})$$

Assuming that $\forall r : 1 - D_{r,11}m \neq 0$ (well-posedness), defining the quantity $\Delta = (1 - D_{r,11}m)$ allows us to express the entries of (A.1) as

$$A_r^\Delta = \rho^{-1} \left(\begin{bmatrix} A & B_{r,1} \\ 0 & 1 \end{bmatrix} + \begin{bmatrix} B_{r,1} \\ 0 \end{bmatrix} \Delta m [C_{r,1} \ D_{r,11}] \right) \quad (\text{A.2a})$$

$$B_{r,1}^\Delta = \rho^{-1} \begin{bmatrix} B_{r,1} \\ 0 \end{bmatrix} \Delta \quad (\text{A.2b})$$

$$B_{r,2}^\Delta = \rho^{-1} \left(\begin{bmatrix} B_{r,2} & \Pi \\ 0 & 1 \end{bmatrix} + \begin{bmatrix} B_{r,1} \\ 0 \end{bmatrix} \Delta m [D_{r,12} \ 0] \right) \quad (\text{A.2c})$$

$$C_{r,1}^\Delta = (1 + D_{r,11}\Delta m) [C_{r,1} \ D_{r,11}] \quad (\text{A.2d})$$

$$C_{r,2}^\Delta = [C_{r,2} \ D_{r,21}] + D_{r,21}\Delta m [C_{r,1} \ D_{r,11}] \quad (\text{A.2e})$$

$$D_{r,11}^\Delta = (L - m) + D_{r,11}\Delta \quad (\text{A.2f})$$

$$D_{r,12}^\Delta = (I + D_{r,11}\Delta m) [D_{r,12} \ 0] \quad (\text{A.2g})$$

$$D_{r,21}^\Delta = D_{r,21}\Delta \quad (\text{A.2h})$$

$$D_{r,22}^\Delta = [D_{r,22} \ 0] + D_{r,21}\Delta m [D_{r,21} \ 0]. \quad (\text{A.2i})$$

The cascade of interconnection between the plant in (A.1) and the filter in (24) is

$$\begin{pmatrix} \hat{A}_r^\lambda & \hat{B}_{r,1}^\lambda & \hat{B}_{r,2}^\lambda \\ \hat{C}_{r,1}^\lambda & \hat{D}_{r,11}^\lambda & \hat{D}_{r,12}^\lambda \\ \hat{C}_{r,2}^\lambda & \hat{D}_{r,21}^\lambda & \hat{D}_{r,22}^\lambda \end{pmatrix} \quad (\text{A.3})$$

$$= \begin{pmatrix} A_f & B_f \hat{C}_{r,1}^\Delta & D_f(\lambda) \hat{B}_{r,1}^\Delta & D_f(\lambda) \hat{B}_{r,2}^\Delta \\ 0 & \hat{A}_r^\Delta & \hat{B}_{r,1}^\Delta & \hat{B}_{r,2}^\Delta \\ C_f(\lambda) & C_f(\lambda) \hat{C}_{r,1}^\Delta & D_f(\lambda) \hat{D}_{r,11}^\Delta & D_f(\lambda) \hat{D}_{r,12}^\Delta \\ 0 & \hat{C}_{r,2}^\Delta & \hat{D}_{r,21}^\Delta & \hat{D}_{r,22}^\Delta \end{pmatrix}.$$

The decision variables involved in the control synthesis Problem 2 are the r -dependent nonlinearly-transformed controller parameters with dimension $\tilde{n} = n + 1 + \nu_{\max}$

$$\mathcal{A}_r \in \mathbb{R}^{\tilde{n} \times \tilde{n}} \quad \mathcal{B}_r \in \mathbb{R}^{\tilde{n} \times 1} \quad (\text{A.4a})$$

$$\mathcal{C}_r \in \mathbb{R}^{2 \times \tilde{n}} \quad \mathcal{D}_r \in \mathbb{R}^{2 \times 1}, \quad (\text{A.4b})$$

the storage function terms

$$\mathcal{P}_r \in \mathbb{S}_{\tilde{n}} \quad \mathcal{J}_r \in \mathbb{R}^{\tilde{n} \times \tilde{n}}, \ \mathcal{H}_r \in \mathbb{S}_{\tilde{n}}, \quad (\text{A.5})$$

and the r -independent quantities

$$\mathcal{X} \in \mathbb{R}^{\tilde{n} \times \tilde{n}}, \quad \mathcal{Y} \in \mathbb{R}^{\tilde{n} \times \tilde{n}}, \quad \mathcal{S} \in \mathbb{R}^{\tilde{n} \times \tilde{n}}. \quad (\text{A.6})$$

The no-algebraic-loop structural constraint in (34) is implemented as the implication

$$D_{r,22} \neq 0 \implies [D_{r,2}]_2 = 0. \quad (\text{A.7})$$

The closed-loop storage function \mathcal{M}_r and slack variable \mathcal{G} have expressions of

$$\mathcal{M}_r := \begin{bmatrix} \mathcal{P}_r & \mathcal{J}_r^\top \\ \mathcal{J}_r^\top & \mathcal{H}_r \end{bmatrix} \quad \mathcal{G} := \begin{bmatrix} \mathcal{X} & \mathcal{S} \\ I_n & \mathcal{Y} \end{bmatrix}. \quad (\text{A.8})$$

The optional restriction to a parameter-independent storage function involves setting

$$\mathcal{S} = I, \quad \forall r \in 1..N_s : \mathcal{P}_r = \mathcal{X}, \ \mathcal{H}_r = \mathcal{Y}, \ \mathcal{J}_r = 0. \quad (\text{A.9})$$

The interconnection of the controller in (A.4) and the plant $G_r^{\lambda 0}$ is

$$\mathcal{A}_{r,cl} = \begin{bmatrix} A_r^\lambda \mathcal{X} + B_{r,2}^\lambda \mathcal{C}_r & A_r^\lambda \mathcal{X} + B_{r,2}^\lambda \mathcal{D}_r \mathcal{C}_{r,2}^\lambda \\ \mathcal{A}_r & \mathcal{Y} A_r^\lambda + \mathcal{B} \mathcal{C}_{r,2}^\lambda \end{bmatrix} \quad (\text{A.10a})$$

$$\mathcal{B}_{r,cl} = \begin{bmatrix} B_{r,1}^\lambda + B_{r,2}^\lambda \mathcal{D}_2 \mathcal{D}_{r,21}^\lambda \\ \mathcal{Y} B_{r,1}^\lambda + \mathcal{B}_r \mathcal{D}_{r,21}^\lambda \end{bmatrix} \quad (\text{A.10b})$$

$$\mathcal{C}_{r,cl} = [C_{r,1}^\lambda \mathcal{X} + D_{r,12}^\lambda \mathcal{C}_r \quad C_{r,1}^\lambda + D_{r,12}^\lambda \mathcal{D}_r \mathcal{C}_{r,2}^\lambda] \quad (\text{A.10c})$$

$$\mathcal{D}_{r,cl} = D_{r,11}^\lambda + D_{r,12}^\lambda \mathcal{D}_r \mathcal{D}_{r,21}^\lambda. \quad (\text{A.10d})$$

The per-edge $(r, r') \in \mathcal{E}$ strict antipassivity relation in (7) is met if the following inequality holds

$$\begin{bmatrix} \mathcal{M}_{r'} & \mathcal{A}_{r,cl} & \mathcal{B}_{r,cl} \\ \mathcal{A}_{r,cl}^\top \mathcal{G} + \mathcal{G}^\top - \mathcal{M}_r & -\frac{1}{2} \mathcal{C}_{r,cl} & \\ \mathcal{B}_{r,cl}^\top & -\frac{1}{2} \mathcal{C}_{r,cl} & -\frac{1}{2} (\mathcal{D}_{r,cl} + \mathcal{D}_{r,cl}^\top) - \epsilon I \end{bmatrix} \succ 0. \quad (\text{A.11})$$

Theorem 10. Under Assumptions 1-5, a ρ -exponentially convergent algorithm can be synthesized if the following program is feasible:

$$\text{find Variables in (A.4)} \quad (\text{A.12a})$$

$$\forall (s, s') \in \mathcal{E} : \text{anti-passivity relation (A.11)} \quad (\text{A.12b})$$

$$\forall s \in 1..s : \text{only gradients (A.7)} \quad (\text{A.12c})$$

Proof. The procedure in (A.10) conducts a nonlinear change of variables in accordance with Section 5.1.1 of De Caigny et al. (2012). Condition (A.11) ensures that the warped plant is ϵ -strictly antipassive.

If the program in (A.12) is feasible, then the controller R_r can be recovered by first computing the no-direct-feedthrough controller R_r^0

$$\mathcal{V} \mathcal{U} = \mathcal{S} - \mathcal{Y} \mathcal{X} \quad (\text{A.13a})$$

$$\begin{bmatrix} A_{r,c}^0 & B_{r,c}^0 \\ C_{r,c}^0 & D_{r,c}^0 \end{bmatrix} = \begin{bmatrix} \mathcal{V}^{-1} & -\mathcal{V}^{-1} \mathcal{Y} B_{r,2}^\lambda \\ 0 & I \end{bmatrix} \begin{bmatrix} \mathcal{A}_r - \mathcal{Y} \hat{A}_r^\lambda \mathcal{X} & \mathcal{B}_r \\ \mathcal{C}_r & \mathcal{D}_r \end{bmatrix} \begin{bmatrix} \mathcal{U}^{-1} & 0 \\ -C_{r,2}^\lambda \mathcal{X} \mathcal{U}^{-1} & I \end{bmatrix} \quad (\text{A.13b})$$

The recovered controller R_r after adding-back the direct feedthrough and reverting the ρ -exponential weighting is

$$\begin{pmatrix} A_{r,c} & B_{r,c} \\ C_{r,c} & D_{r,c} \end{pmatrix} = \begin{pmatrix} \rho^{-1} (A_{r,c}^0 - B_{r,c}^0 D_{r,c}^0 C_{r,c}^0) & \rho^{-1} (B_{r,c}^0) \\ (I - D_{r,c}^0 D_{r,22}) C_{r,c}^0 & D_{r,c}^0 \end{pmatrix}, \quad (\text{A.13c})$$

because the no-algebraic-loop constraint (34) ensures that $I - D_{r,22} D_{r,c}^0 = I$. The controller R_r from (A.13c) is then connected to the relevant plants to yield the controller $K_r = Q_r \star R_r$ and the optimization algorithm $P_r \star Q_r \star R_r$.

REFERENCES

- Ahmadi, A.A., Jungers, R.M., Parrilo, P.A., and Roozbehani, M. (2014). Joint Spectral Radius and Path-Complete Graph Lyapunov Functions. *SIAM Journal on Control and Optimization*, 52(1), 687–717.
- Apkarian, P., Gahinet, P., and Becker, G. (1995). Self-scheduled H-infinity control of linear parameter-varying systems: a design example. *Automatica*, 31(9), 1251–1261.
- Bianchi, M., Ananduta, W., and Grammatico, S. (2021). The distributed dual ascent algorithm is robust to asynchrony. *IEEE Control Systems Letters*, 6, 650–655.

- Boczar, R., Lessard, L., and Recht, B. (2018). Exponential Convergence Bounds Using Integral Quadratic Constraints. In *American Control Conference*.
- Briat, C., Sename, O., and Lafay, J.F. (2009). Delay-scheduled state-feedback design for time-delay systems with time-varying delays—a LPV approach. *Systems & Control Letters*, 58(9), 664–671.
- Conte, G., Perdon, A., Zattoni, E., and Animobono, D. (2021). Disturbance decoupling and model matching problems for discrete-time systems with time-varying delays. *Nonlinear Analysis: Hybrid Systems*, 41, 101043.
- Conte, G., Perdon, A.M., and Zattoni, E. (2020). Modeling discrete time systems with variable delays as switching systems without delays. In *2020 European Control Conference (ECC)*, 1591–1594. IEEE.
- De Caigny, J., Camino, J.F., Oliveira, R.C., Peres, P.L., and Swevers, J. (2012). Gain-scheduled dynamic output feedback control for discrete-time LPV systems. *Int. J. Robust Nonlinear Control.*, 22(5), 535–558.
- De Oliveira, M.C., Geromel, J.C., and Bernussou, J. (2002). Extended H_2 and H_∞ norm characterizations and controller parametrizations for discrete-time systems. *International Journal of Control*, 75(9), 666–679.
- Desoer, C.A. and Vidyasagar, M. (1975). *Feedback Systems: Input-Output Approach*. Academic Press, London.
- Doostmohammadian, M., Khan, U.A., Pirani, M., and Charalambous, T. (2021). Consensus-based distributed estimation in the presence of heterogeneous, time-invariant delays. *IEEE Control Systems Letters*, 6, 1598–1603.
- Francis, B.A. and Wonham, W.M. (1976). The internal model principle of control theory. *Automatica*, 12(5), 457–465.
- Gahinet, P. and Nemirovskii, A. (1993). General-Purpose LMI solvers with benchmarks. In *Proc. IEEE Conf. Decis. Control*, 3162–3165 vol.4.
- Gripenberg, G. (1996). Computing the joint spectral radius. *Linear Algebra and its Applications*, 234, 43–60.
- Holicki, T. and Scherer, C.W. (2021). Algorithm design and extremum control: Convex synthesis due to plant multiplier commutation. In *Proc. IEEE Conf. Decis. Control*, 3249–3256. IEEE.
- Jakob, F. and Iannelli, A. (2025). A Linear Parameter-Varying Framework for the Analysis of Time-Varying Optimization Algorithms. *arXiv preprint arXiv:2501.07461*.
- Köroğlu, H. (2012). Generalized asymptotic regulation for lpv systems with additional performance objectives. In *Control of Linear Parameter Varying Systems with Applications*, 127–156. Springer.
- Köroğlu, H. and Scherer, C.W. (2008). LPV control for robust attenuation of non-stationary sinusoidal disturbances with measurable frequencies. *IFAC Proceedings Volumes*, 41(2), 4928–4933.
- Lessard, L., Recht, B., and Packard, A. (2016). Analysis and design of optimization algorithms via integral quadratic constraints. *SIAM Journal on Optimization*, 26(1), 57–95.
- Megretski, A. and Rantzer, A. (1997). System analysis via Integral Quadratic Constraints. *IEEE Transactions on Automatic Control*.

- Michalowsky, S., Scherer, C., and Ebenbauer, C. (2021). Robust and structure exploiting optimisation algorithms: an integral quadratic constraint approach. *International Journal of Control*, 94(11), 2956–2979.
- Mohammadi, H., Razaviyayn, M., and Jovanović, M.R. (2021). Robustness of Accelerated First-Order Algorithms for Strongly Convex Optimization Problems. *IEEE Transactions on Automatic Control*.
- Ramaswamy, A., Redder, A., and Quevedo, D.E. (2021). Optimization over time-varying networks and unbounded information delays. *IEEE Transactions on Automatic Control*, 67(8), 4131–4137.
- Scherer, C. and Ebenbauer, C. (2021). Convex synthesis of accelerated gradient algorithms. *SIAM Journal on Control and Optimization*, 59(6), 4615–4645.
- Scherer, C.W. (2023). Robust exponential stability and invariance guarantees with general dynamic o’shea-zames-falb multipliers. *IFAC-PapersOnLine*, 56(2), 5799–5804. 22nd IFAC World Congress.
- Scherer, C.W., Ebenbauer, C., and Holicki, T. (2023). Optimization algorithm synthesis based on integral quadratic constraints: A tutorial. In *Proc. IEEE Conf. Decis. Control*, 2995–3002. IEEE.
- Stoorvogel, A.A., Saberi, A., and Sannuti, P. (2000). Performance with regulation constraints. *Automatica*, 36(10), 1443–1456.
- Van Scoy, B., Freeman, R.A., and Lynch, K.M. (2017). The fastest known globally convergent first-order method for minimizing strongly convex functions. *IEEE Control Systems Letters*, 2(1), 49–54.
- Wen’an, Z., Li, Y., and Hongbo, S. (2008). A switched system approach to networked control systems with time-varying delays. In *2008 27th Chinese Control Conference*.